Published in final edited form as:
Langmuir. 2007 April 24; 23(9): 5045–5049. doi:10.1021/la063765e.

Multiscale Structure of the Underwater Adhesive of *Phragmatopoma Californica*: a Nanostructured Latex with a Steep Microporosity Gradient

Mark J. Stevens, **Rebekah E. Steren**, **Vladimir Hlady**, and **Russell J. Stewart***
Department of Bioengineering, University of Utah, Salt Lake City, Utah 84112

Abstract

Phragmatopoma Californica builds a tubular dwelling by gluing bits of sand and seashell together underwater with a proteinaceous adhesive. In the lab, the animals will build with 0.5 mm glass beads. Two spots of glue with a consistent volume of about 100 pL each are deposited on the glass beads before placement on the end of the tube. The animals wriggled the particles for 20-30 s before letting go, which suggested that the adhesive was sufficiently set within 30 s to support the glass beads. The structure of the adhesive joints was examined at the micro- and nanoscopic length scales using laser scanning confocal and atomic force microscopies. At the microscale, the adhesive was a cellular solid with cell diameters ranging from 0.5 to 6.0 μm, distributed to create a steep porosity gradient that ranged from near zero at the outside edges to about 50% at the center of the adhesive joint. At the nanoscale, the adhesive appeared to be an accretion of trillions of deformable nanospheres, reminiscent of a high-solids-content latex adhesive. The implications of the structure for the functionality of the adhesive is discussed.

Introduction

Phragmatopoma californica is a gregarious tube-dwelling marine polychaete that lives in the intertidal zone off the coast of California in sandcastlelike colonies.1,2 *Phragmatopoma* have a distinctive strategy for building their tubular homes. Rather than secreting a mineralized shell, they gather preformed mineral particles from the water column that they glue together into a composite tube. The worms build with both inorganic sand grains and biogenic shell fragments of the correct size to fit within their building organs, about 0.5 mm. The building organ is a pulpy, crescent-shaped organ where the proteinaceous glue that holds the composite shell together is secreted. In several species of tube-dwelling polychaetes similar to *Phragmatopoma* that have been studied extensively,3-6 the glue appears to issue from bouquets of glandular cells located within the thorax of the worms. The glandular cells produce morphologically distinct secretory granules, described as homogeneous and heterogeneous,4 that range in size from 1.5 to 5 μm in diameter. The secretory granules travel up through ductlike extensions of the glandular cells, through a muscular band, to where they appear to be combined, mixed, and applied as small dabs to the mineral particles held in the building organ. The dabs of glue cure into flexible, leathery material that has the structure of a solidified foam.7 The ability of this proteinaceous glue to adhere to a mélange of mineral substrates and to hold together a robust shell capable of

*To whom correspondence should be addressed. E-mail: rstewart@eng.utah.edu..

Supporting Information Available: Videos showing *P. californica* gluing particles onto its shell and a through focus series of laser scanning confocal microscope images. This material is available free of charge via the Internet at http://pubs.acs.org.

withstanding the high-energy environment of the intertidal zone makes it an intriguing model for bioadhesive and antifouling research.

The *P. californica* glue is comprised of at least three proteins, referred to as Pc1-3,8,9 and significant amounts of Mg^{2+} and Ca^{2+}.7 There may be additional as yet-unidentified components. All three proteins have highly repetitive and blocky primary structures with limited amino acid diversity. Pc1 (18 kDa) is dominated by glycine (G, 45 mol %), lysine (K, 14 mol %), and tyrosine (Y, 18.7 mol %), which occur in multiple copies of the consensus sequence block, LGGYGYGGKK. Pc1 is basic (pI 9.74) due to the absence of acidic residues and the presence of a high proportion of K. Pc2 (21.1 kDa) also has a repetitive primary structure predominated by G (27.5 mol %), alanine (A, 19 mol %), Y (9 mol %), and histidine (H, 9 mol %) occurring in interspersed repeats of the sequence HPAXHK where X is usually V, and ALGGYGAGA. Pc2 is also basic (pI 9.91). Pc3 exists in at least two major variants, Pc3a (13.9 kDa), and Pc3b (30.5 kDa), both of which are rich in serine (S, 72.9 mol %) and Y (10 mol %). Pc3 is a remarkably acidic protein (pI 0.5-1.5) because the S residues are phosphorylated.7 The Y residues, scattered fairly evenly throughout all three proteins, are post-translationally hydroxylated to form di-hydroxyphenylalanine (DOPA). The presence of DOPA in the glue is significant because it readily undergoes oxidative crosslinking into higher-order congeners. DOPA has been identified in the byssal plaques of mussels10 where it is thought to play two primary roles: first, to facilitate solidification through di-DOPA cross-link formation between precursor proteins11,12 and, second, to improve adhesion to mineral substrates.13 DOPA residues may play similar roles in the glue of *P. californica*.

A bonding mechanism for the *P. californica* glue has been proposed largely on the basis of its liquid-filled foam structure and composition.7 A central tenet of the model is that the oppositely charged proteins and divalent cations may coalesce into an electrically neutralized, liquid-liquid foam through the process of complex coacervation—the spontaneous separation of a solution containing polyelectrolytes into two immiscible, aqueous phases.14,15 pH may play a critical role in setting the glue. At the acidic pH of secretory granules (5.2) the coacervated glue solution may have a viscosity and low interfacial tension that facilitates spreading on wet mineral substrates as it is secreted. As the secreted droplet of glue equilibrates to the pH of seawater (8.2) it may harden due to two mechanisms: the change in bonding between Ca^{2+} and phosphate from electrostatic to ionic at elevated pH and covalent cross-linking between DOPA and nucleophilic residues, in particular cysteine residues.9 The studies reported here provide additional details about the micro- and nanoscale structure of the *P. californica* glue.

Materials and Methods

Time-Lapse Video Recording

P. californica colonies were collected from sites near Goleta, CA, shipped overnight to Salt Lake City, UT, and maintained in an artificial seawater environment. An individual animal was removed from the colony and placed in a beaker containing 0.5 mm glass beads, bovine cortical bone fragments, or 0.5 mm silicon particles diced from 0.5 mm thick silicon wafers. After allowing the animal to build overnight, a notch was formed near the top of the tube to prompt localized repair of the tube and the animal was replaced onto a bed of substrate particles. Time lapse video was recorded using a Hitachi KP-D50 color Digital Camera with both analog and digital outputs and a Panasonic AG-6730 Time Lapse VCR. Videos spanned a 12 h period following notch creation in the tube. Particle setting times were recorded and tallied from three different videos.

Cement Disk Harvest

Individual sand tubes containing a single animal were carefully removed from the colony by hand, and after separation the portion nearest the animal's operculum was removed. The animals were placed, unharmed and with approximately 3/4-1 in. of original shell, into 250 mL flasks onto a bed of 0.5 mm diameter glass beads which had been previously rinsed in seawater filtered with 0.22 μm regenerated cellulose filters. The animals were left overnight to rebuild their tubes. After 24 h the portion of the tube made of glass beads was removed with forceps and the animals were replaced onto their bed of glass beads for 24 more hours. The most solid of the cement disks, those found nearest the original tube, could be removed with forceps from the glass beads. Intact cement disks were collected into 1.7 mL Eppendorf tubes containing filtered seawater. For laser scaning confocal microscopy studies the glue disks were immediately wet-mounted onto glass microscope slides and sealed with fingernail polish. For AFM studies glue disks were kept in the Eppendorf tubes until they were mounted on a round glass coverslip.

Laser Scanning Confocal Microscopy

Confocal microscopy was performed at the Cell Imaging Core Microscopy Facility at the University of Utah using an Olympus Fluoview FV 300 laser scanning confocal microscope with computer-controlled stage. To elicit fluorescence, 488 nm excitation was used, and 2048 × 2048 pixel images were collected with a 60× oil emersion objective with a two-pass Kalman filter. The glue disk's autofluorescence allowed visualization of the glue without staining. The pores were dark. Optical sections of the cement disks were taken with 0.3 μm *z*-axis spacing.

Confocal Image Processing

Confocal images were processed with Image J software (NIH). First, a fast Fourier transform bandpass filter was applied to the images to delineate edge features in the cement disk images. Afterward, a median bandpass filter was used to smooth the image. The thresholding function was used to create a binary image of the disks in which the fluorescent material appeared white and pores appeared black. The outline of the glue disk was traced, and the area of the glue disk measured. Afterward, the part of the image not containing the glue disk was cut away. A particle analysis function in Image J was used to count and measure the pore area in each image. By multiplying the pore area by the distance between the images the volumes of the glue disks and pores were calculated.

The glue disks were concave on both sides due to the spherical nature of the glass bead substrate. The concavity of the glue disks created a problem when studying porosity with repect to distance from the glue/substrate interface because a single image in the *X*-*Y* plane showed a slice in which the distance to the nearest glue/substrate interface was a function of the distance from the center of the glue disk. Consequently, in the studies of porosity with respect to distance from the glue/substrate interface radial sections were used rather than an image of the entire glue disk. Radial sections allowed us to easily subdivide and examine the image with respect to distance from the center of the whole disk. Three radial sections of two glue disks were used to examine porosity with respect to distance from the interface.

Atomic Force Microscopy

Freshly harvested fully cured glue disks adhered to glass beads were analyzed by AFM in both wet and dry states. Dry glue disks were first rinsed in distilled water, frozen, lyophilized (Labconco), broken apart, and analyzed in air. It was previously demonstrated using scanning electron microscopy that dried glue disks fractured cohesively.7 For wet analysis, beads with adhered glue disks were mounted in filtered seawater in a fluid cell.

When glued beads are broken apart in the wet state the adhesive bond generally fails adhesively. All disks were examined with a Nanoscope II (Veeco) atomic force microscope in contact mode using a silicon nitride tip. Data were represented using WsXM v2.1 software. The *z*-axis scale from the WsXM-rendered AFM images was used to estimate the volume of the individual structures. Images from wet or dry glue disks were highly similar with regard to nanoparticle shapes and sizes.

Results and Discussion

Adhesive Set Times

By patiently watching several worms glue dozens of particles onto their tubes we are able to make the first estimates of the initial set time of the *P. californica* glue. Three different *P. californica* worms were recorded for ~12 h as they rebuilt their tubes with either glass beads or bovine cortical bone fragments. Dozens of events were observed in which the worms, after positioning new particles on the edge of their tube, wriggle the particles back and forth with their building organ as if checking the set before releasing the particle (Figure 1A and B, Supporting Information). The wriggling motion could also play a role in mixing the newly deposited glue. With glass beads, bovine cortical bone fragments, or diamond-shaped particles of silicon as substrate, the glue was sufficiently set within 30 s to be released (Table 1). The dabs of glue are initially milky white but turn reddish-brown over a period of several hours and developed the consistency of leather (Figure 1C).

Microscale Structure

The glue disks recovered from glass bead substrates were roughly circular, often in a nearly closed horseshoe shape, and concave on both surfaces that were in contact with the spherical glass beads (Figure 2). The glue is strongly autofluorescent across the entire visible spectrum, making structural characterization by laser scanning confocal microscopy convenient (Supporting Information). On glass beads, the glue disks had characteristic dimensions demonstrating that the worm secretes a consistent volume of glue to form each adhesive joint (Table 2). The glue disks were about 150 μm in diameter and 15 μm thick. The total volume of the glue disks was calculated by summing the volumes (measured surface area by step displacement between sections) of optical sections obtained by laser scanning confocal microscopy. The glue disks had a volume of about 100 pL, corresponding to a contact area of about 1.2×10^{-2} mm^2 per dab of glue. Glue dabs applied to less regularly shaped particles, like bovine cortical bone fragments, spread to fill the spaces between particles and thus were not regularly shaped and were difficult to recover for structural characterization.

The set glue has a mixed cell solid foam structure. The cells ranged in diameter from 0.4 to 6.5 μm. The total porous volume of each optical section was calculated by summing the dark areas within each section and multiplying by the thickness. The average total porosity for the glue disks was around 25% (Table 2). An apparent porosity gradient can be seen in electron micrographs of lyophilized glue disks,7 as well as in three-dimensional reconstructions of the porous volume from confocal optical sections (Figure 2). The *x*-axis porosity gradient, from bead interface to bead interface as diagrammed in Figure 3A, was quantified by determining the average porosity of each *x*-axis optical section. The radial gradient was quantified by measuring the average porosity at three positions along a radius extending from the glue centroid of each *x*-axis optical section (Figure 3A). This analysis demonstrated that the fully set *P. californica* glue does indeed have steep porosity gradients from the center of the glue toward the interfaces with the glass bead substrates, as well as from the center toward the outer edges exposed to seawater (Figure 3B). The porosity ranges from as high as 50% near the center of the glue disk to nearly zero at the exposed edge.

The gradient may be simply due to the fluid-filled bubbles of the liquid foam self-organizing by size in the double concave space between the glass spheres. Indeed, simple experiments with wet soap foams and round-bottom flasks produce qualitatively similar soap bubble gradients. Alternatively, if the glue sets from the outside surface that first comes into contact with seawater inward, the solidifying glue could drive the water-filled pores toward the fluid center of the glue disk. Or, somewhat slower setting in the center of the glue disk due to a slower pH shift may allow more time for water-filled pores to coalesce into larger pores. Whatever the mechanism, the porosity gradient suggests a remarkably efficient use of its adhesive by *P. californica*. Analysis of stress distributions on adhesive joints under tensile or shear loading has shown that maximum stresses occur at the edges of the joints.16 Under shear loading, induced cleavage stress normal to the load at the edge of the joint are actually greater than the shear stress.17 One of the practical consequences of the uneven stress distributions in adhesive joints under shear is that if 50% of the area in the center of a lap joint is unbonded there is a mere 3% decrease in joint strength.18 A similar effect is expected for *P. californica* adhesive joints. The happy consequence of the *P. californica* adhesive gradient is to concentrate material at the edges where the stresses are maximal and to spare material in the center of the joint where stresses are minimal, thus creating the highest quality joint while saving vital metabolic energy.

Nanoscale Structure

When probed at the nanometer scale using AFM, the *P. californica* glue was found to be composed of 50-100 nm globular structures (Figure 4). Nanopores occur in the interstices of the closely packed globules. We note two other examples of natural protein-based adhesives that have been observed to have globular nanostructures, barnacle adhesive on nonstick surfaces20 and the adhesive secreted by frogs of the genus *Notaden*.21 The flattened interfaces and 120° angles characteristic of Plateau borders observed in high-resolution AFM images of the *P. californica* glue (Figure 4C) suggest the nanoparticles were deformable at the time the glue was secreted onto the substrate. A complete understanding of the forces responsible for the deformations requires further investigation, such as determining the magnitude of the deformations at different regions of the adhesive disks. One set of forces could be adhesion between the particles that prevent the freshly secreted glue from dispersing into the seawater counterbalanced by elastic deformations that resist complete coalescence.19 Elastic and/or plastic deformations of the *P. californica* adhesive nanoparticles could play an important role in strengthening the joint by absorbing and dissipating strain energy and in particular the cleavage strains concentrated at the edges. With deformable nanoparticles to absorb tensile strains and the open cell microstructure acting as micro-dashpots to absorb compressive shocks, the *P. californica* adhesive appears to have multiscale energy absorbing systems that helps cope with life in the high-energy enviroment of the intertidal zone.

A model that adds new details to the earlier models7,9 of the *P. californica* adhesive structure and bonding mechanisms is presented in Figure 5. The oppositely charged proteins (Pc1-3) and divalent Ca^{2+} and Mg^{2+} cations condense through electrostatic interactions into a nanoparticulate aqueous phase (complex coacervation) in secretory cells of the cement glands. The effect of complex coacervation is to concentrate the adhesive proteins into a high-solids-content, yet fluid, latex. The cohesive forces between particles in the fluid may be mediated by divalent cations bridging excess negative surface charges and/or by interparticle diffusion of protein molecules. As the secretions of multiple secretory cells coalesce into an adhesive bolus in cement gland ducts, fluid-filled vacuoles may be entrapped, creating the microporous foam structure of the adhesive. The final secreted latex solution is denser than seawater, sufficiently viscous and cohesive to prevent rapid

dissolution into the surrounding seawater, but flowable with a low interfacial tension that allows spreading and crack filling on the wet mineral surface.

The setting mechanism likely exploits the pH differential between secretory vesicles (pH 5) and seawater (pH 8.2). One potential pH trigger mechanism is a change in the nature of the bonding between Ca^{2+} and/or Mg^{2+} with the phosphate sidechains of Pc3 from electrostatic interactions to stronger more specific ionic interactions at the higher pH of seawater. Although knowledge of the form and stoichiometry of the Ca/Mg in the *P. californica* glue requires further study, this may be a plausible mechanism to account for the observed rapid initial set of the adhesive (Table 1). A second pH-triggered mechanism may be formation of quinone-based intermolecular and interparticle cross-links between the DOPA residues evenly distributed throughout all three glue proteins. DOPA in the oxidized quinone form can homocouple to form di-DOPA cross-links or undergo nucleophilic attack by lysine or cysteine residues.22 Evidence of cysteinyl-DOPA residues in the *P. californica* adhesive has been reported.9 The reddish-brown coloration of the cement that develops over several hours is also consistent with the presence of cysteinyl-DOPA-based pigments in the glue.23 The spontaneous coupling between cysteine and DOPA would be accelerated at the elevated pH of seawater because the deprotonated thiol of cysteine is a stronger nucleophile than the protonated form. The quinone-based covalent crosslinking may continue for several hours and be responsible for the tough leathery consistency of the fully cured adhesive.

To lend further credence to the complex coacervation model, we point to another example of a species that builds elaborate nanostructured foams starting with the complexation of polyphosphates and polyamines into nanoparticles. Diatoms are single-celled photosynthetic organisms that secrete amorphous glass shells. The highly porous shells can be described as precisely organized foams within foams. The shells are composites of silica and matrix proteins called silaffins.24 At nanometer resolution,25 the apparently solid matrix surrounding the microscale pores is seen to consist of nanoparticles reminiscent of the nanospheres shown in Figure 4. Like the *P. californica* glue proteins, the silaffin matrix proteins are highly charged due to a high proportion of phosphoserines and amines.24 A current model for diatom shell formation posits that silaffins, associated (coacervated) through electrostatic interactions, nucleate the polymerization of silicic acid (SiO_4) into silica nanoparticles, which then phase-separate to form the precise solid foam structure of the shell.26,27

Conclusion

Although much remains to be learned about the *P. californica* adhesive, it is clear that some of the most important features of modern synthetic structural adhesives have been put into practice by marine invertebrates for tens of millions of years. Perhaps as additional details of the mechanism are uncovered the *P. calfornica* glue will provide a valuable model for designing robust water-based underwater adhesives for biomedical and other applications.

Supplementary Material

Refer to Web version on PubMed Central for supplementary material.

Acknowledgments

We thank Dr. Larry deVries for helpful discussions. This work was supported by a Funding Incentive Seed Grant from the University of Utah Research Foundation.

References

(1). Eckelbarger, K. Metamorphosis and settlement in the sabellariidae. In: Rice, ME., editor. Settlement and Metamorphosis of Marine Invertebrate Larvae. Elsevier North-Holland Biomedical Press; Amsterdam: 1978.

(2). Jensen RA. Marine bioadhesive: role for chemosensory recognition in a marine invertebrate. Biofouling. 1992; 5(3):93.

(3). Gruet Y, Vovelle J, Grasset M. Bioinorganic components in the tube cement of Sabellaria alveolata (L.) annelid polychete. Can. J. Zool. 1987; 65(4):837–42.

(4). Vovelle J. Organic-mineral cement from Petta pusilla Malmgren, Polychete tubicole. C. R. Seances Acad. Sci. 1979; 288(21):1599–602.Ser. D

(5). Vovelle J. The tube of *Salbellaria alveolata*. Arch. Zool. Exp. Gen. 1965; 106:1–187.

(6). Truchet M, Vovelle J. Study of the cement glands of a tubicolous polychaete (Pectinaria (=Lagis) koreni) with the help of electron microprobe and ion microanalyzer. Calcif. Tissue Res. 1977; 24(3):231–6. [PubMed: 597762]

(7). Stewart RJ, Weaver JC, Morse DE, Waite JH. The tube cement of Phragmatopoma californica: A solid foam. J. Exp. Biol. 2004; 207(26):4727–4734. [PubMed: 15579565]

(8). Waite JH, Jensen RA, Morse DE. Cement precursor proteins of the reef-building polychaete Phragmatopoma californica (Fewkes). Biochemistry. 1992; 31(25):5733–8. [PubMed: 1610822]

(9). Zhao H, Sun C, Stewart RJ, Waite JH. Cement Proteins of the Tube-building Polychaete Phragmatopoma californica. J. Biol. Chem. 2005; 280(52):42938–42944. [PubMed: 16227622]

(10). Waite JH, Tanzer ML. Polyphenolic Substance of *Mytilus edulis:* Novel Adhesive Containing L-Dopa and Hydroxyproline. Science. 1981; 212:1038–1040. [PubMed: 17779975]

(11). Waite JH. Reverse engineering of bioadhesion in marine mussels. Ann. N. Y. Acad. Sci. 1999; 875:301–309. (Bioartificial Organs II). [PubMed: 10415577]

(12). Sever MJ, Weisser JT, Monahan J, Srinivasan S, Wilker JJ. Metal-mediated cross-linking in the generation of a marine-mussel adhesive. Angew. Chem., Int. Ed. 2004; 43(4):448–50.

(13). Waite JH, Qin X. Polyphosphoprotein from the Adhesive Pads of Mytilus edulis. Biochemistry. 2001; 40(9):2887–2893. [PubMed: 11258900]

(14). Bundenberg de Jong, HG. Morphology of Coacervates. In: Kruyt, HR., editor. Colloid Science. Vol. 2. Elsevier Publishing Company; Amsterdam: 1949. p. 431-482.Reveraible Systems

(15). Bundenberg de Jong, HG. Crystallization - coacervation - flocculation. In: Kruyt, HR., editor. Colloid Science. Vol. 2. Elsevier Publishing Company; Amsterdam: 1949. p. 232-255.Reversible Systems

(16). Lacombe, R. Adhesion measurement methods: theory and practice. CRC Press; Boca Raton, FL: 2006.

(17). Goland M, Reissner E. The stresses in cemented joints. J. Appl. Mech. 1944; 11:17–27.

(18). deVries, KL.; Borgmeier, PR. Fracture mechanics analyses of the behavior of adhesive test specimens. In: Van Ooij, WJ.; Anderson, HR., editors. Mittal Festschrift. VSP; Leiden, The Netherlands: 1998. p. 615-640.

(19). Israelachvili JN. Adhesion forces between surfaces in liquids and condensable vapours. Surf. Sci. Rep. 1992; 14:109–159.

(20). Wiegemann M, Watermann B. Peculiarities of barnacle adhesive cured on non-stick surfaces. J. Adhes. Sci. Technol. 2003; 17(14):1957–1977.

(21). Graham LD, Glattauer V, Huson MG, Maxwell JM, Knott RB, White JW, Vaughan PR, Peng Y, Tyler MJ, Werkmeister JA, Ramshaw JA. Characterization of a protein-based adhesive elastomer secreted by the Australian frog Notaden bennetti. Biomacromolecules. 2005; 6(6):3300–12. [PubMed: 16283759]

(22). Burzio LA, Waite JH. Cross-Linking in Adhesive Quinoproteins: Studies with Model Decapeptides. Biochemistry. 2000; 39(36):11147–11153. [PubMed: 10998254]

(23). Ito S, Novellino E, Chioccara F, Misuraca G, Prota1 G. Copolymerization of dopa and cysteinyldopa in melanogenesis in vitro. Cell. Mol. Life Sci. 1980; 367:822–823.

(24). Kroger N, Deutzmann R, Sumper M. Polycationic peptides from diatom biosilica that direct silica nanosphere formation. Science. 1999; 286(5442):1129–32. [PubMed: 10550045]

(25). Noll F, Sumper M, Hampp N. Nanostructure of Diatom Silica Surfaces and of Biomimetic Analogues. Nano Lett. 2002; 2(2):91–95.

(26). Kroger N, Lorenz S, Brunner E, Sumper M. Self-assembly of highly phosphorylated silaffins and their function in biosilica morphogenesis. Science. 2002; 298(5593):584–6. [PubMed: 12386330]

(27). Sumper M. A phase separation model for the nanopatterning of diatom biosilica. Science. 2002; 295(5564):2430–3. [PubMed: 11923533]

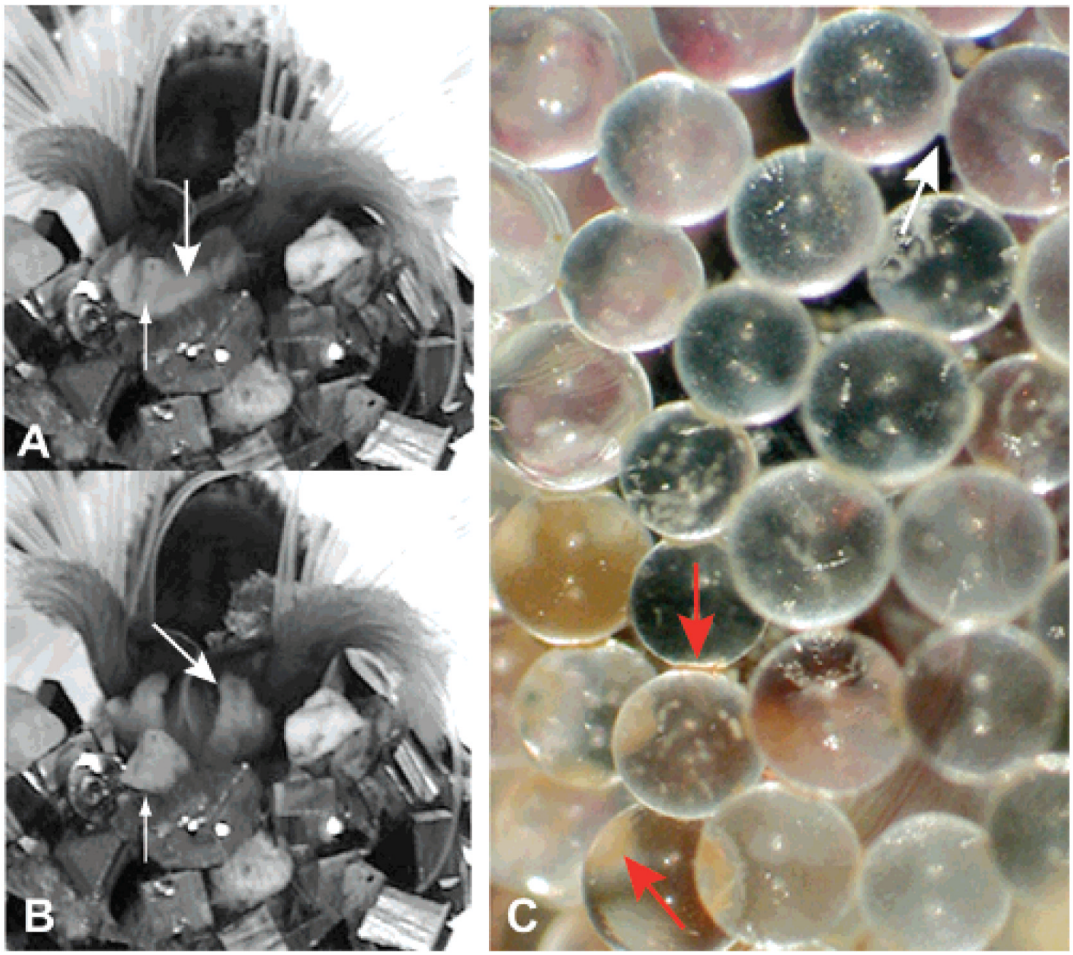

Figure 1.
P. californica adding a sand grain to its tube. (A) After applying dabs of glue, *P. californica* nestles a sand grain into place and holds it for 20-30 s before letting go. (B) Building organ. Large arrows indicates the building organ after release of a sand grain. Small arrows indicate the freshly adhered sand grain. (C) When freshly deposited, the glue is creamy white (white arrow). After several hours, the glue turns rusty brown in color (red arrows).

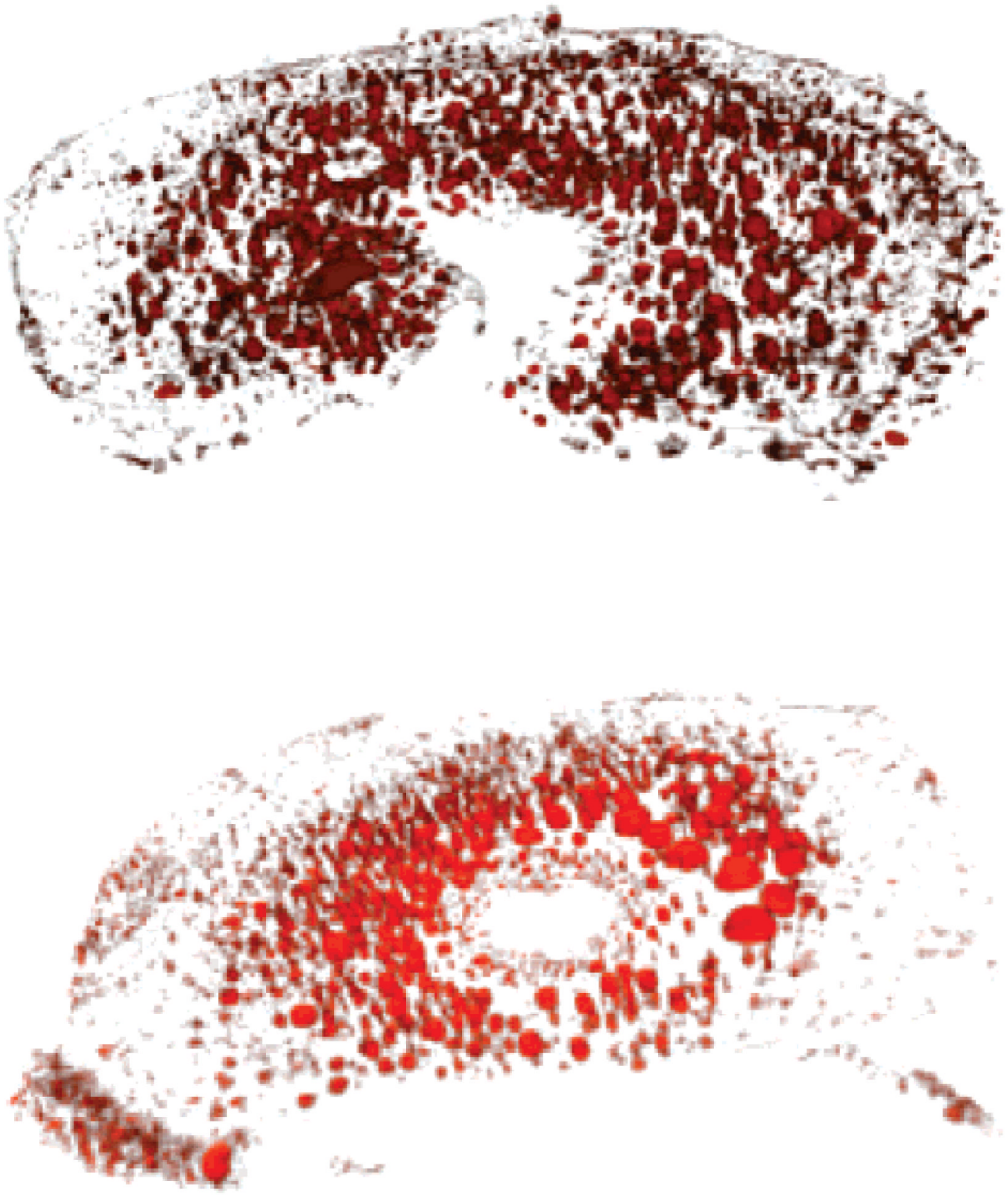

Figure 2.
Porous volume of two representative glue disks rendered in three dimensions by reconstructing laser scanning confocal microscopy optical sections. The nearly solid edges and higher porous central regions are evident.

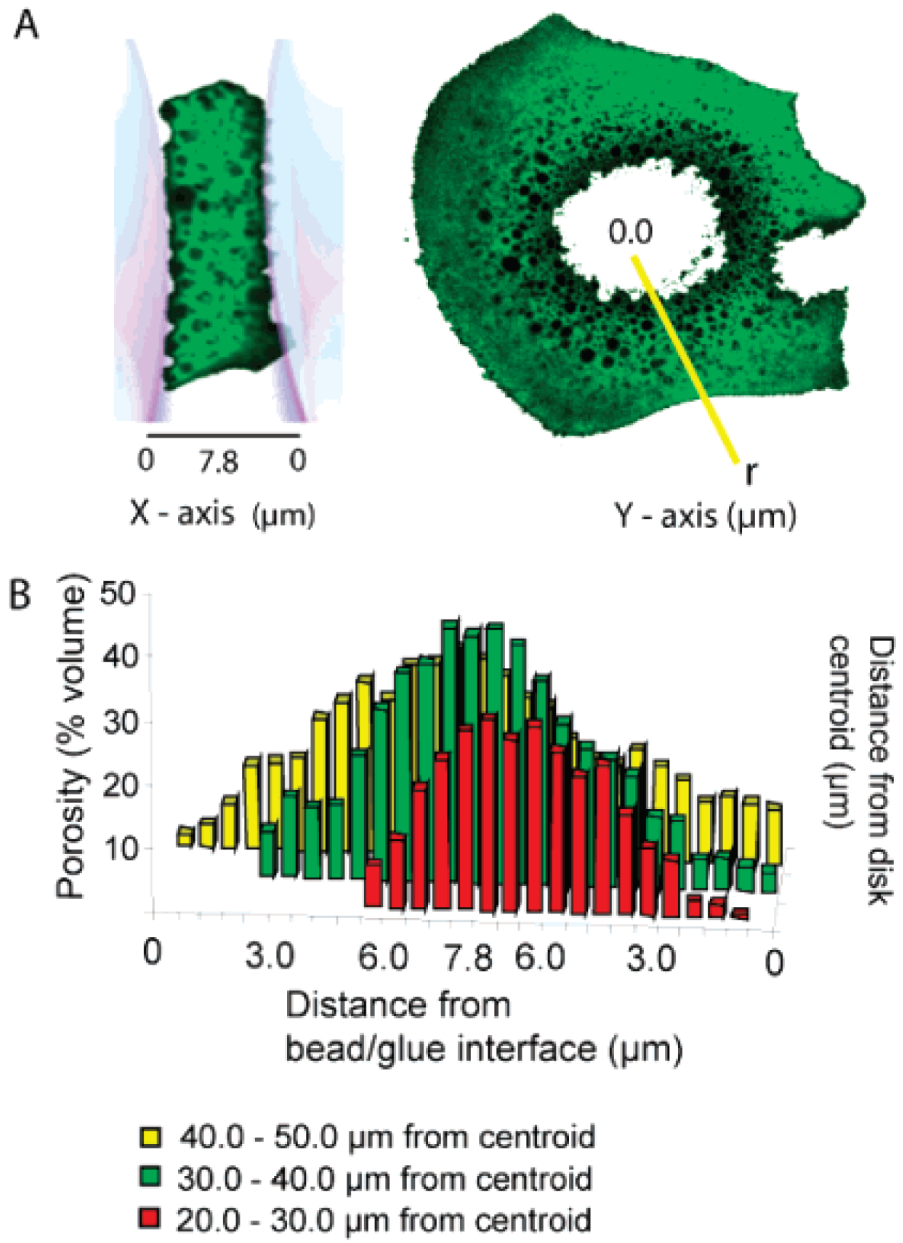

Figure 3.

Porosity (*Z*-axis) measured as a function of distance from glue-substrate interface (*X*-axis) and as a function of distance (*r*) from the centroid of the glue disk (*Y*-axis). (A) Representative confocal fluorescent images of glue disks and definition of porosity plot axes. (B) Porosity varies as a function of distance from the glue/bead interface and as a function of radial distance (*r*) from the centroid. For clarity error bars were not added to the bar graph; errors in all cases were less than 10%.

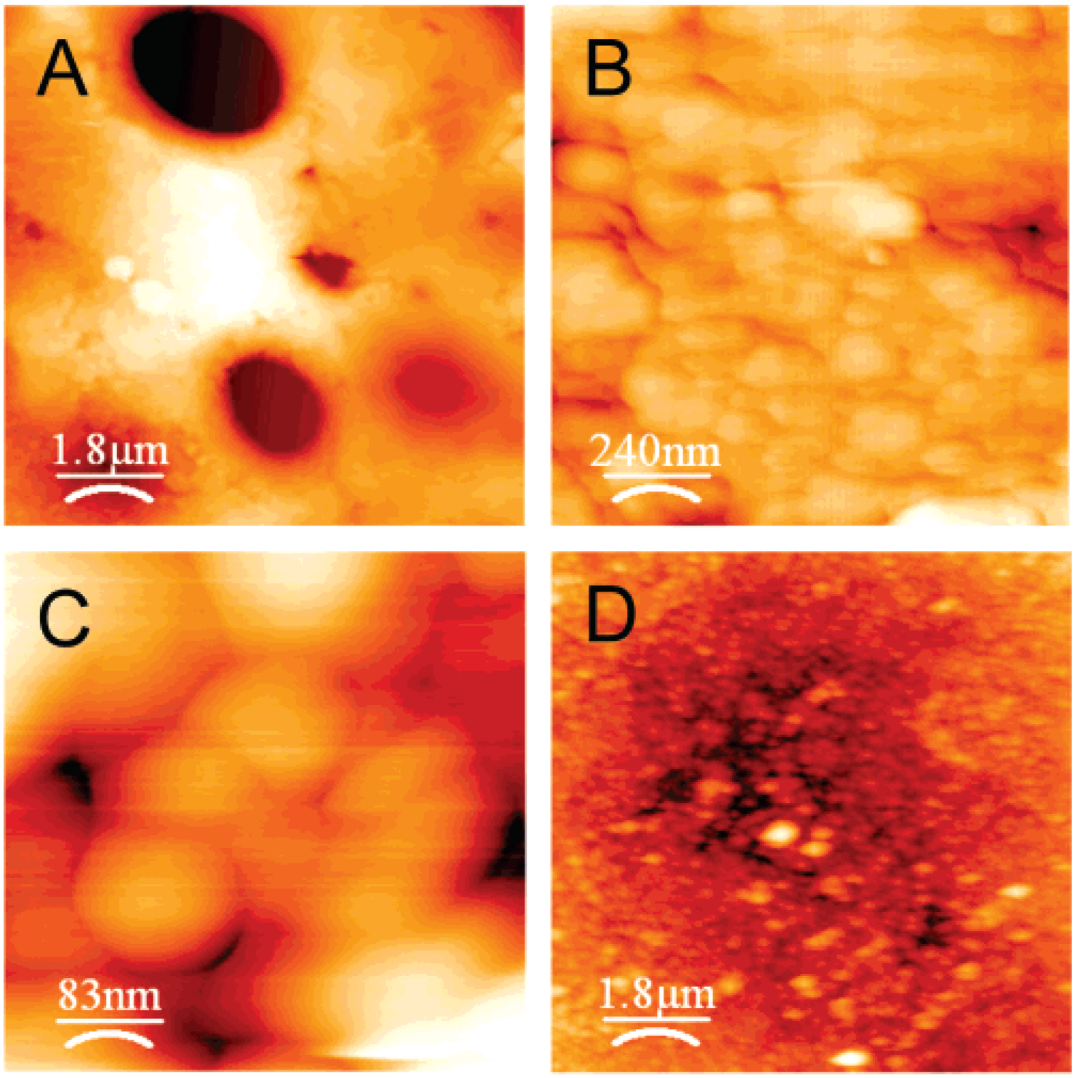

Figure 4.
Representative AFM images of *P.californica* glue. (A-C) Dried and cohesively fractured glue disks at increasing resolution. (D) Hydrated glue disk.

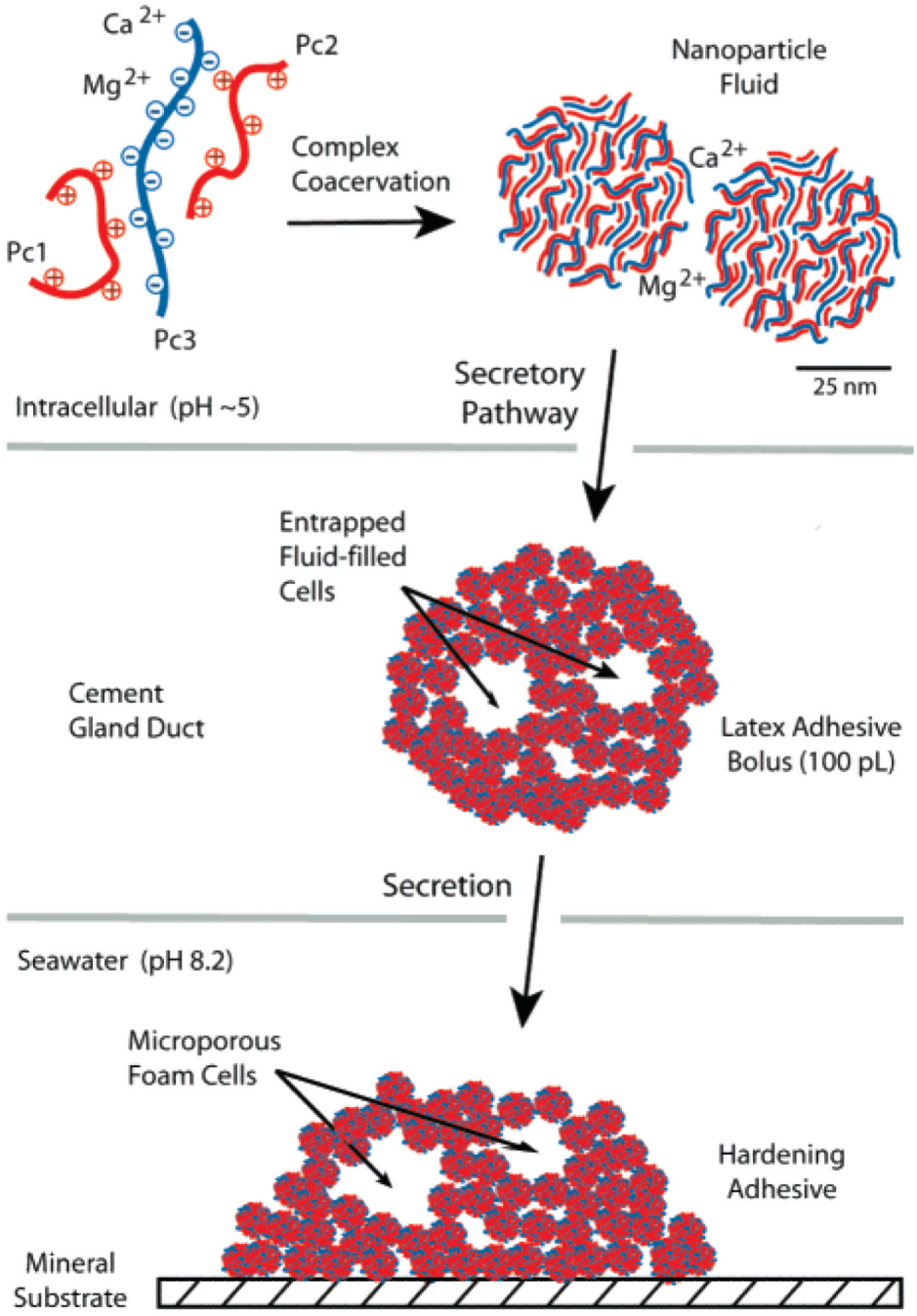

Figure 5.

P. californica adhesive model. Within secretory cells of the cement glands a mixture of the oppositely charged adhesive proteins (Pc1-3) and divalent cations condense into a nanoparticulate fluid phase through complex coacervation. Initial adhesion between the deformable nanoparticles may be mediated by electrostatic bridging of excess negative surface charges by divalent cations and strand exchange between particles. When secreted, the high-solids-content adhesive latex is denser than seawater, has sufficient viscosity and cohesion to prevent rapid dissolution into the seawater, but low interfacial tension to allow spreading and crack filling on the wet mineral substrate. A discontinuous aqueous phase trapped in the setting adhesive forms a microporous foam structure. A two-stage curing

mechanism may be initiated by the pH differential between secretory vesicles (pH 5) and seawater (pH 8.2). The first stage is rapid (~30 s) and may be mediated by a change in the nature of the bonding of divalent cations with phosphate sidechains of Pc3, from nonspecific electrostatic interactions to more specific ionic bonds. A second, slower hardening to form a tough leathery adhesive may occur through quinonic cross-linking between DOPA and cysteine residues.

Table 1

Adhesive Set Times with Three Types of Substrate

substrate	average set time (s)
glass microspheres	22.8 ± 7.5 (*n* = 85)
silicon	29.7 ± 5.8 (*n* = 32)
bovine cortical bone	23.5 ± 5.3 (*n* = 30)

Table 2

Glue Disk Dimensions and Porosity Determined by Laser Scanning Confocal Microscopy

disk	disk diam (μm)	disk thickness (μm)	disk vol (pL)	av porosity[a]	av pore diam (μm)	pore diam range (μm)
1	143.9	16.2	97.4	31	1.2	0.4-4.9
2	166.3	15.6	105.5	27	2.9	0.7-4.5
3	169.4	8.4	103.8	27	1.5	0.4-6.0
4	133.6	15.3	95.9	18	2.0	0.8-4.4

[a]Percent of total disk volume.